EXPERIMENTAL AND NUMERICAL INVESTIGATION OF HEAT TRANSFER IN BATTERY PACK OF A HOVERBOARD

BY

ABHINAV PRASAD

Presented to the Faculty of the Graduate School of

The University of Texas at Arlington in Partial Fulfillment

Of the Requirements

For the Degree of

MASTER OF SCIENCE IN MECHANICAL ENGINEERING

THE UNIVERSITY OF TEXAS AT ARLINGTON

MAY 2018

Copyright © by Abhinav Prasad 2018

All Rights Reserved

Acknowledgements

I am very grateful for the opportunity to work with many brilliant and meticulous individuals during this degree. I would like to begin by thanking Dr Ankur Jain for giving me the opportunity to join his group in Microscale Thermophysics Laboratory. He has been a truly inspirational teacher. I learned a great deal from our interactions from past couple of semesters.

I am grateful to Dr. Ratan Kumar and Dr. Miguel Amaya for being my committee members and evaluating my thesis work.

Help from everyone in MTL lab is greatly appreciated. I would especially like to thank Hardik Prajapati, Mohammad Parhizi and Darshan Ravoori for their continued support and guidance during my thesis.

I would like to thank Mr. Kermit Beird for helping me in fabrication of parts.

Finally, I thank my parents Mr. S.D. Prasad and Mrs. S. Prasad for all their love and support.

This material is based upon work supported by CAREER Award No. CBET 1554183 from the National Science Foundation.

April 26, 2018

ABSTRACT

EXPERIMENTAL AND NUMERICAL INVESTIGATION OF HEAT TRANSFER IN BATTERY PACK OF A HOVERBOARD

Abhinav Prasad, MS

The University of Texas at Arlington, 2018

Supervising Professor: Ankur Jain

Li-ion cells are used for energy storage and conversion in electric vehicles and a variety of consumer devices such as hoverboards. Performance and safety of such devices is severely affected by overheating of Li-ion cells in aggressive operating conditions. Several accidents due to fire in the battery pack of a hoverboard have been reported in the recent past. Despite the large number of hoverboards in use worldwide, there is a lack of systematic research on heat transfer in battery packs of hoverboards. This study presents experimental and numerical analysis of heat transfer in Li-ion battery pack of a hoverboard to understand the effect of natural and forced cooling on the temperature of the battery pack. Experiments conducted on a roller conveyor set-up show that surface temperature of the cells improves by

removing the metal casing around the pack and by providing openings on the hoverboard. A finite element simulation model is developed, the results of which are in good agreement with experimental data for both natural and forced convection. Experimental data and simulations indicate the need of removing the metal casing in addition to providing external air flow. The simulation model also indicates that providing holes in the casing can result in significant thermal benefit without the need to remove the casing completely. Results of this work improve our understanding of heat transfer in hoverboards and may contribute towards improved safety of hoverboards.

Table of Contents

List of Figures

Chapter 1

INTRODUCTION

Temperature directly affects the safety, reliability and performance of several energy systems relevant for energy conversions. One such energy conversion device is a Li-ion cell. It's used as an energy storage and conversion in a wide variety of engineering applications such as electric vehicles, laptops, mobile phones, hoverboards etc. [1-3]. However, Li-ion cells are temperature sensitive [5,6] and its performance significantly reduces at high and low temperature. One such disadvantage of exposure to high temperature is fast aging and accelerate capacity fade. In addition, overheating of Li-ion cells also presents significant reliability and safety challenges, due to the risk of thermal runaway [7,8].

Management of heat effects associated with Li-ion cells remains a challenge because of heat generation within the cells which may lead to thermal runaway of individual cells or of an entire battery pack. Since cells are tightly packed in a battery pack, thermal runaway of a single cell can blow up an entire battery pack. One such device that uses tightly packed cells is a hoverboard. A hoverboard is a low speed mobility device used for personal transportation. In the past, many cases of fire and explosion due to hoverboard were reported. Most of it were originated in battery pack. Almost in all cases, only one side, which contains battery pack, of the hoverboard was burnt.

A significant amount of research has been carried out to understand the fundamental heat transfer characteristics of a single Li-ion cell [9-12], as well as battery packs consisting of multiple Li-ion cells [13-16]. At the scale of a single cell, direction-dependent thermal conductivity has been measured [9-12]. Heat generation due to electrochemical reactions inside the cell has been characterized [17-18]. Overall rate of heat generation in the cell has been determined through electrochemical [19] as well as calorimetric measurements [10]. Thermal runaway in a single Li-ion cell has been studied extensively in a variety of abuse conditions [18,19], through both experiments and theoretical analysis [11,20].

Much work has also been carried out on thermal measurements and theoretical modelling of battery packs, although most work has been limited to large battery packs of relevance to electric vehicles [14-16]. Active and passive cooling has been investigated through experiments and numerical analysis [21]. Air and liquid based cooling technique have been studied both experimentally and numerically [22,23]. A water-based hydrogel thermal management approach has been studied to handle the heat surge during the operation of a Li-ion battery pack [23]. The use of liquid cooling plates has also been investigated for battery packs [24]. Phase change material has been used to improve the thermal performance of battery pack in electric scooters [14, 25, 26]. A combination of aluminium foam and phase change material has been studied for improved heat transfer. A novel hybrid thermal management technique that combines phase change material and

forced cooling has been demonstrated for electric vehicle battery pack [27]. Experimental investigation of thermal management using heat pipe has been carried out in an electric vehicle [28, 29]. A few research papers have utilized finite element simulations to investigate the thermal performance of a battery pack [30,31,32]. Numerical modelling of battery pack of laptops by using phase change material has been carried out [30] and expanded graphite has been impregnated in the phase change material to improve thermal conductivity [30].

In contrast to the sizable literature on thermal phenomena in cells and battery packs for electric vehicles summarized above, there is relatively lesser work on thermal design and management of smaller battery packs for devices such as hoverboards. While the power requirement or total energy stored in a small battery pack such as in a hoverboard may not be as large as an electric vehicle, a systematic study of thermal management of these battery packs is clearly necessitated by the large number of hoverboards in use and the critical need to ensure consumer safety. Further, unlike in an electric vehicle, the number of thermal management options may be limited in a hoverboard due to size and cost considerations, making it even more important to optimize heat transfer within these constraints to minimize peak temperature rise and hence the risk of thermal runaway. A combination of experimental measurements and theoretical/numerical investigation is likely to be an effective approach towards this goal.

This work presents experimental measurements and numerical analysis of thermal management of the Li-ion battery pack of a hoverboard. A hoverboard is disassembled and instrumented to measure Li-ion cell temperatures during nominal operating conditions. Measurements indicate significant temperature rise and risk of thermal runaway in present conditions. Cooling of the battery pack with air flowing relative to the moving hoverboard is investigated by providing cut-outs in the frame to permit air flow into the battery pack. This, along with removal of a metal casing around the pack is shown to result in 33% reduction in cell temperature rise compared to the present case. Experimental data are found to be in good agreement with results from finite element simulations. Experiments and simulations indicate that the metal casing that houses the battery pack plays a key role in determining the effectiveness of thermal management. The provision of perforations on the casing is shown to result in reasonable reduction in temperature rise without compromising the structural function of the casing. Experimental data presented here demonstrate the thermal benefit of using the relative speed of air around the moving hoverboard for cooling for the battery pack. This does not require any fan work since the air flow is generated due to hoverboard motion. The experimentally validated numerical simulation results from this work may be useful as a predictive design tool for improved performance and thermal safety of hoverboards.

Chapter 2

Hoverboard Construction

Hoverboard is a self-balancing scooter used for personal transportation. It weighs around 22 lbs and it can withstand maximum weight of 100 kg. It has a dimensions of 23 by 4 by 7 inch and its pedal height is 4.3 inch from ground level. It has two hard rubber tire and 2 motors are integrated inside the wheels. Figure 1 shows an assembled hoverboard.

Figure 1: Image showing an assembled hoverboard.

It has two compartments, which are covered with a 2 mm thick plastic cover. After removing the plastic panel, one side of the hoverboard consists of battery management system, battery pack and a metal casing and these parts are mounted on an aluminum chassis of thickness 3 mm. Figure 2 shows one side of hoverboard which houses above mentioned parts. It also has multiple wires that are used to connect battery management system to motherboard.

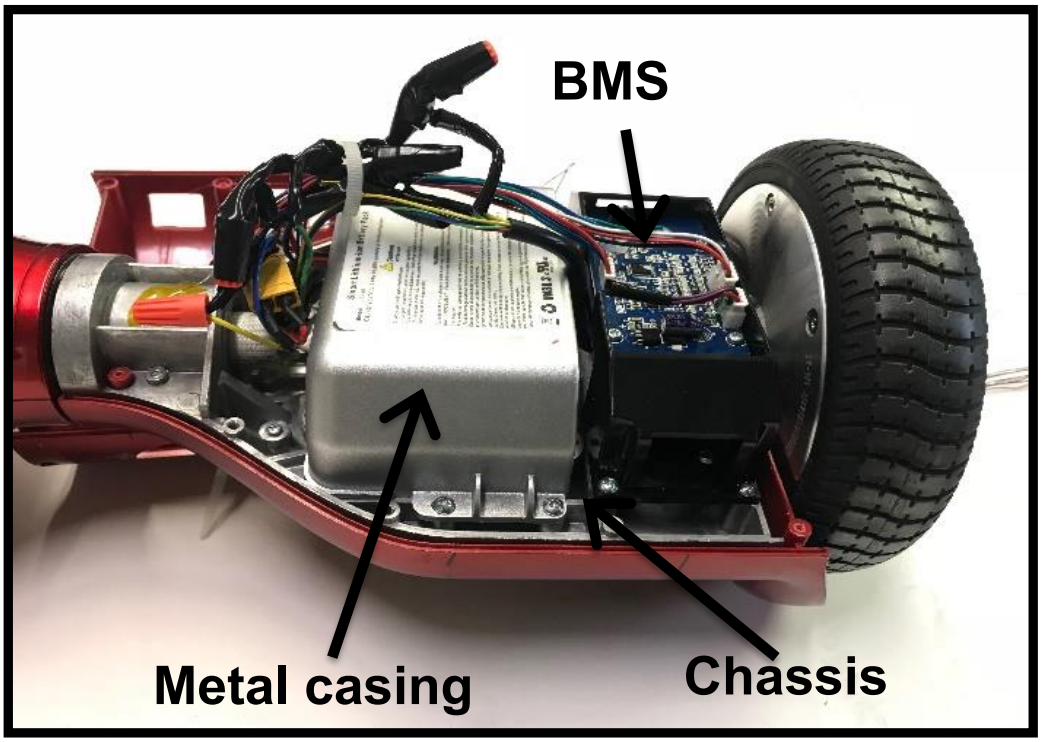

Figure 2: Image showing one side of hoverboard that houses BMS, metal casing, wirings and chassis.

Other side of the hoverboard consists of motherboard, charger and power cable and gyroscope. Above mentioned parts are shown in Figure 3.

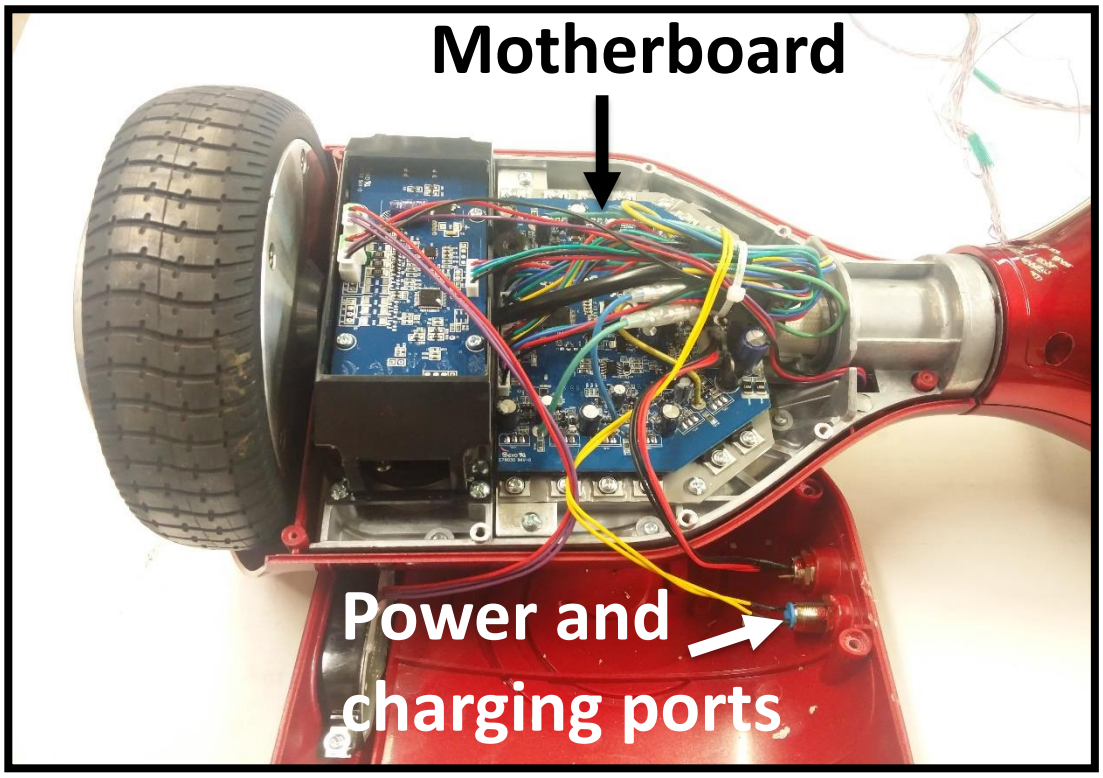

Figure 3: Image showing other side of hoverboard that houses motherboard, charger and power cable, wirings and gyroscope.

Chapter 3

Experiments

Experiments are carried out to measure the temperature of the cells. Since the size of the battery pack is small, cells are tightly packed. Lack of physical access to the cells and the mobile nature of the hoverboard pose challenges in such a measurement. Experiments are designed and carried out to address these challenges and to investigate possible thermal management strategies to reduce temperature rise in the battery pack. This section describes components of the experimental setup, disassembly and the experimental procedure for validation.

3.1. Hoverboard disassembly and instrumentation

The hoverboard is carefully dis-assembled for obtaining physical access to the battery pack. The plastic panel on the right side of the hoverboard is first removed (Figure 4(a)), revealing the battery management system and a metal casing that houses the battery pack (Figure 4(b)). To place thermocouples on cells in the battery pack, the metal casing is carefully removed. To facilitate this, multiple wires that connect the battery management system to the motherboard are cut and reconnected using wire connectors after the metal casing is removed. The battery pack inside the casing, shown in Figure 4(c), comprises 22 tightly packed 18650

cells that are held together by a thin plastic wrap, also shown in Figure 1(c)**.** One face of the cell, insulated by the plastic wrap, touches the metal casing. The assembly of the cells within the battery pack is shown schematically in Figure 5. Note that Figure 2 also shows cut-outs for forced air cooling investigated in experiments and simulations in this work to reduce cell temperature. There is no active cooling mechanism for the battery pack, which loses heat only through natural convection to the surrounding air and through thermal conduction into the metal casing. The battery pack is not disassembled further, since it may not have been possible to assemble it back together. T-type thermocouple wires are placed on nine cells that are physically accessible without disassembling the battery pack **(**Figure 1(d)). Thermocouple wires are routed out of the metal casing and the outer plastic cover and connected to a National Instruments NI-9213 data acquisition system (DAQ), which is controlled by LabView software running on a 64-bit computer. Temperature data are acquired once every second during the discharge process. The disassembly and instrumentation of the battery pack with thermocouples reveals key features on the battery side of the hoverboard, such as the metal casing and plastic wrap around the battery pack that play a key role in determining its thermal performance. Information obtained from this process also enables accurate set up of geometrical models for finite element simulations.

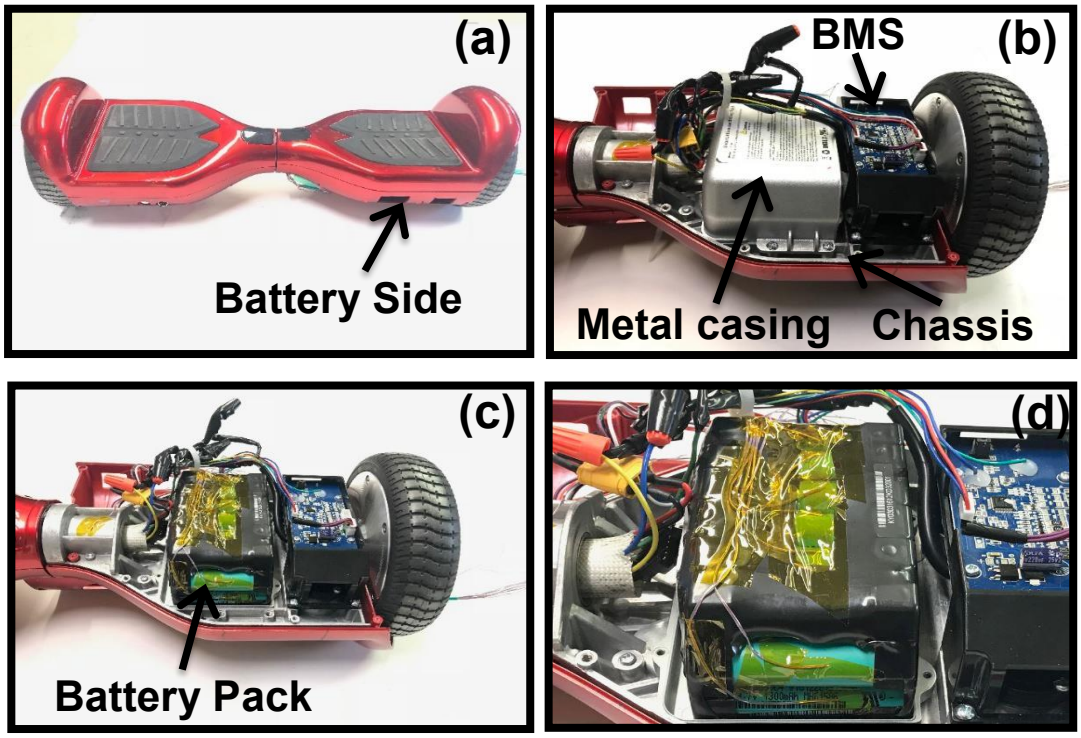

Figure 4: (a)-(c) Pictures from disassembly process of the battery pack side of the hoverboard, showing key internal features including metal casing, plastic wrap and the battery pack. (d) Picture showing the instrumentation of cells in the battery pack

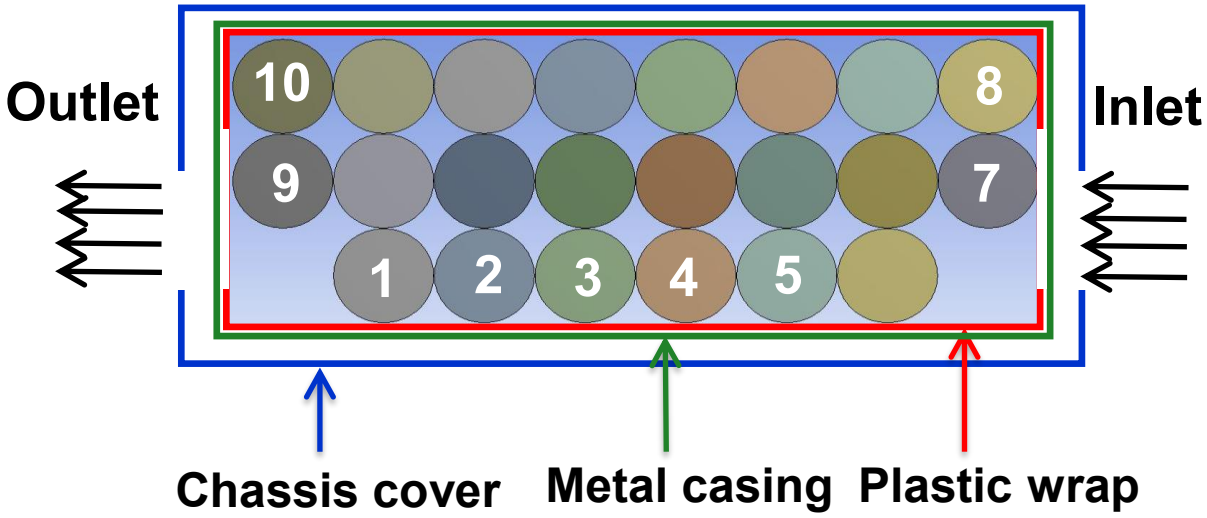

Figure 5: Schematic of the assembly of the cells in the battery pack, also showing the plastic wrap and metal casing around the cell assembly, as well as inlet and outlet grills for mimicking the use of air flow generated by hoverboard motion for cooling

3.2. Fabrication of roller set-up

It is difficult to collect temperature data while hoverboard is in motion. It gets tough to carry a laptop and run a hoverboard at the same time. To overcome this challenge and ensure data acquisition in consistent discharge conditions, a roller conveyor setup is designed and fabricated. Roller conveyor set up consists of 2 steel rollers of diameter 35 mm and length 765 mm that are mounted on a

rectangular metal frame of dimension 770 mm by 200 mm. Figure 6 (a) shows roller set up and figure 6 (b) shows hoverboard placement on roller set up.

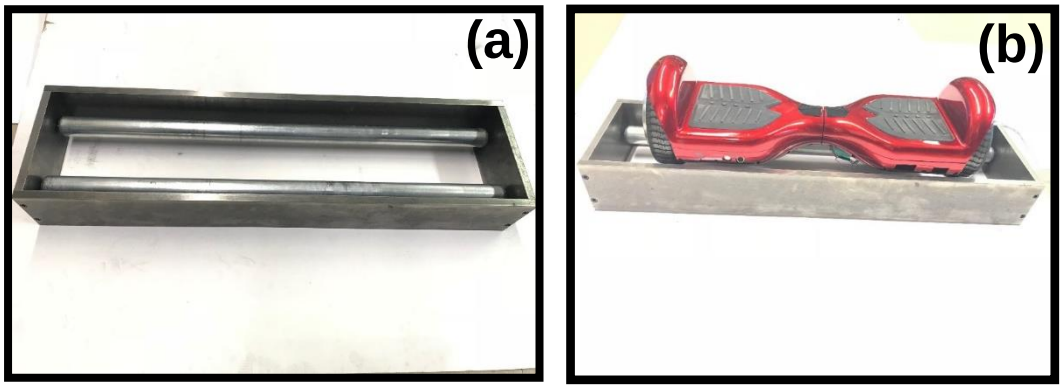

Figure 6: (a) Image of fabricated roller set-up. (b) Image of placement of hoverboard on roller set-up.

3.3. Data acquisition during charging

Temperature measurements are carried out while charging. Hoverboard is fully charged in 2 hours. To ensure proper functioning of the cut off mechanism, which ensures hoverboard is fully charged, total time for the test is 8 hours.

3.4. Hoverboard experimental set up and data acquisition

All measurements are carried out while running the hoverboard on the roller set up. The hoverboard is mounted on the rollers during measurements. By rotating the metal rollers, this setup keeps the hoverboard stationary during measurements,

which greatly simplifies data acquisition and application of air flow for thermal management. Figure 7(a) shows a picture of the experimental setup, including the hoverboard mounted on the roller conveyor setup as well as the data acquisition system. Even though hoverboard motion generates flow of air relative to the hoverboard, this does not effectively cool the battery pack, which is inaccessible to the air flow. To investigate the potential thermal benefits of the air flow on the battery pack, inlet and outlet grills of dimension 100 mm by 35 mm are cut on the plastic casing of the hoverboard, as shown in Figure 7(b). These grills facilitate the flow of air generated due to hoverboard motion into and out of the battery pack. Since the hoverboard in these experiments remains stationary on the roller conveyor setup, the flow of air is mimicked by placing a small fan placed external to the hoverboard to investigate forced air cooling of the battery pack. In order to correctly mimic real conditions, air speed from the fan is chosen to match the measured speed of the hoverboard in nominal operating conditions. The fan is placed about 100 mm from the inlet grill, through which air passes into the inside of hoverboard. The location of the inlet and outlet grills with respect to the cells in the battery pack is shown schematically in Figure 5. Experiments are done at 30 kg and 70 kg load. For 30 kg load, experiment is done only at baseline condition i.e. no grills. For 70 kg load, experiments are first carried out in baseline conditions without any cooling, which represents the present state-of-the-art. Experiments are also carried out in the presence of cooling air from the external

fan that mimics the use of air flow relative to the moving hoverboard for battery pack cooling.

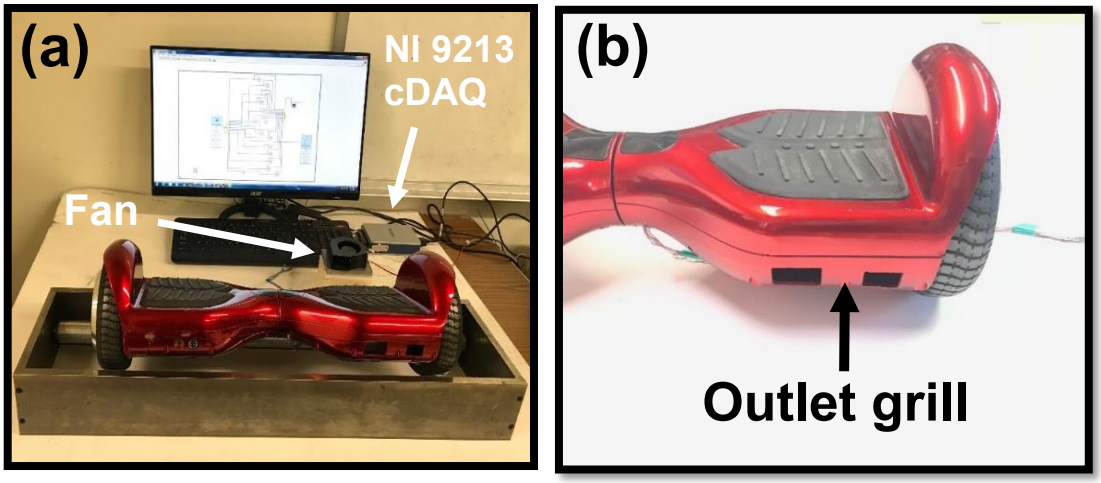

Figure 7: (a) Picture of the experimental setup showing the hoverboard, cooling fan and data acquisition setup. (b) Picture of the outlet grill on the outer plastic body of the hoverboard. The inlet grill, not visible, is on the opposite face.

Chapter 4

Numerical Modelling

The transient temperature field in the battery pack and hoverboard is computed by numerically solving the underlying energy conservation equations using the finite element method in a commercial software tool. The geometry of the hoverboard is obtained from measurements on the disassembled hoverboard. This model consists of hollow plastic casing of 2 mm thickness with a dimension of 240 by 200 mm. Chassis of 3 mm thickness is mounted inside hollow plastic casing. This model consists of battery management system, battery pack which is protected with a plastic wrap of 0.5 mm thickness. Metal casing is used to protect battery pack. Battery pack consists of 22 18650 cells.

Key thermal parameters that influence the temperature field in the hoverboard include heat generation rate and thermal properties of the cells. In addition, thermal properties of other components such as plastic wrap, BMS and metal casing are also important. Heat generation rate of Li-ion cells is known to be a function of the discharge rate [10]. In this work, the discharge rate is first determined based on the time taken during experiments for the battery pack to fully discharge, starting from a fully charged state. Heat generation rate for the present experiments is then determined from past work where heat generation rate

has been measured at different C-rates through measurement of temperature rise and heat flux out of the cell [10]. Heat generation rate is assumed to be constant throughout the discharge process. It is not possible to directly measure the thermal conductivity of the specific cells in the hoverboard's battery pack since the cell cannot be extracted out of the pack. Thermal conductivity of the Li-ion cells is taken to be 0.20 W/mK and 30.4 W/mK in the radial and axial directions respectively, based on past measurements on 18650 Li-ion cells, which is the same cell type as used in the hoverboard. Natural convection cooling with a convective heat transfer coefficient of 10 W/m^2K is assumed for simulations of cases with no forced air. For forced air cooling, fluid flow is modeled with a velocity boundary condition at the inlet. The inlet air speed is obtained from direct measurements from an anemometer. A mesh of 857307 nodes is utilized for finite element computations. Mesh independence is ensured by establishing minimal change in computed temperature field because of further mesh refinement. Figure 8 shows the simulation model which consists of different parts such as plastic cover, chassis, BMS, 22 cells, plastic wrap and metal casing. Figure 9 shows model for forced convection. In this model a velocity of 4 m/s is provided on the inlet grill. Inlet and outlet grills are of dimension 100 by 32 mm.

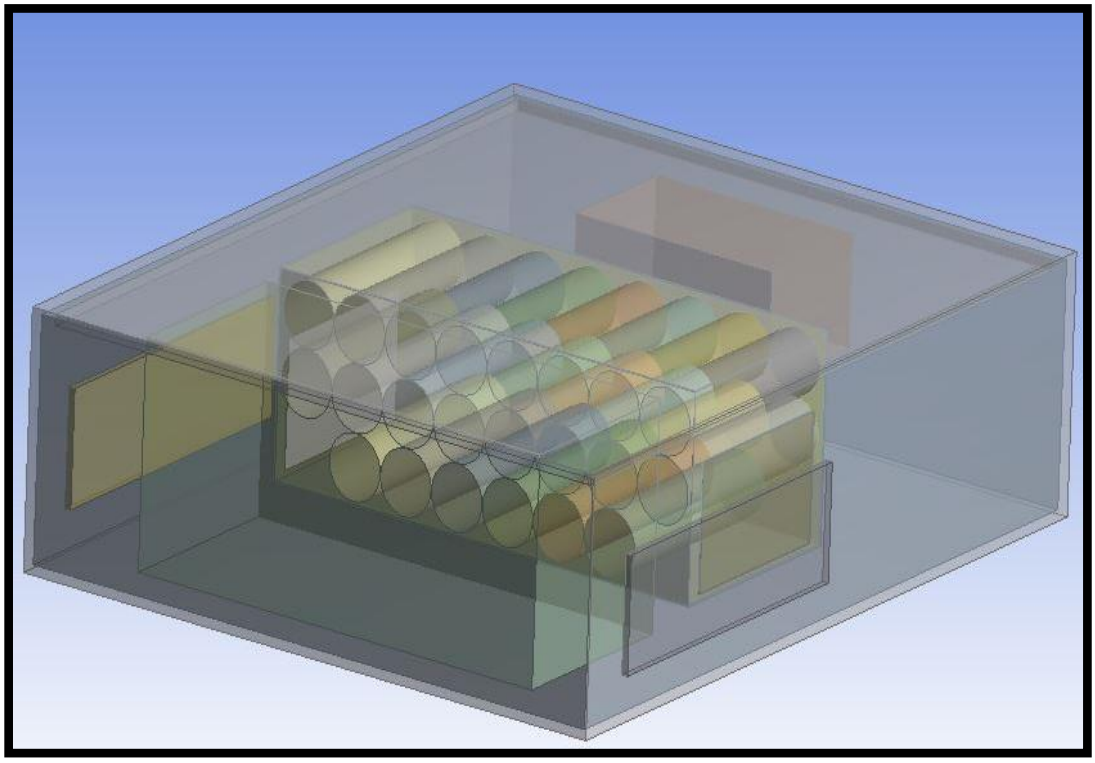

Figure 8: Image showing simulation model for natural convection, which consists of parts such as plastic cover, BMS, chassis, battery pack with plastic wrap and a metal casing.

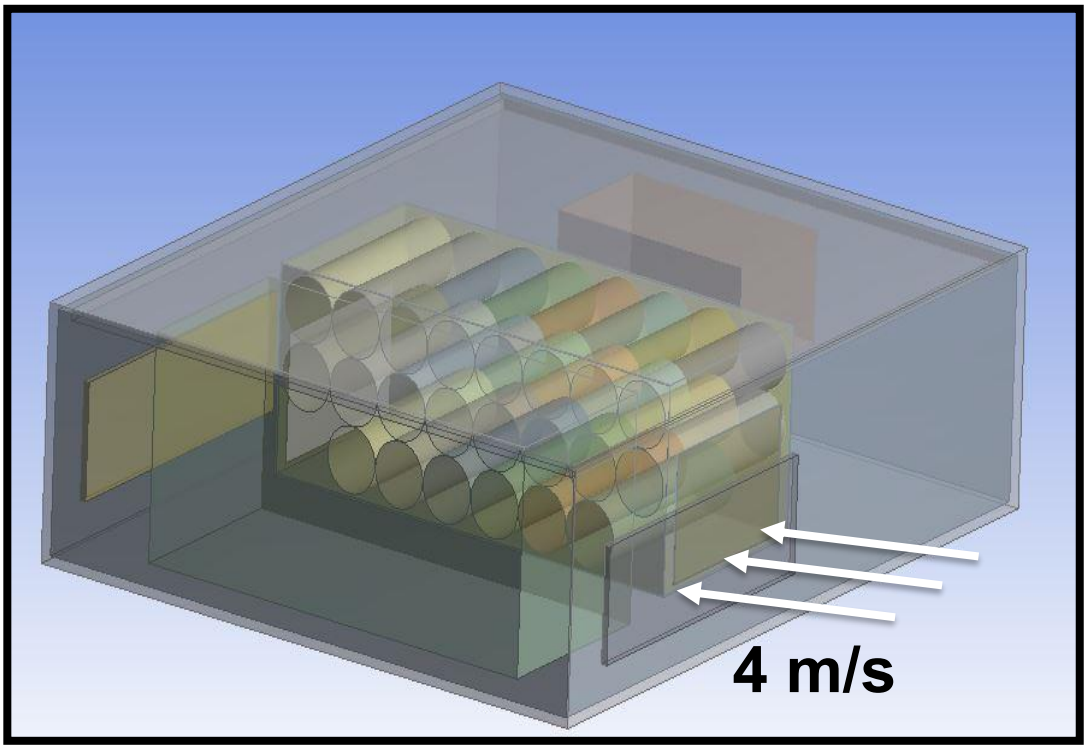

Figure 9: Image showing simulation model for forced convection, which consists of parts such as plastic cover, BMS, chassis, battery pack with plastic wrap, a metal casing and inlet and outlet grills.

Chapter 5

Results

5.1. Temperature Measurements while charging

Figure 1 to 3 present temperature rise at the surface of nine cells during charging. Hoverboard is plugged in for 7 hours to see whether cut-off mechanism in charger kicks on. There is uniform temperature rise in all cells for 2 hours and after that there is drop in temperature for all cells. This indicates the onset of cut-off mechanism in the charger. Figure 10, 11 and 12 show the temperature measurement for all cells for 7 hours.

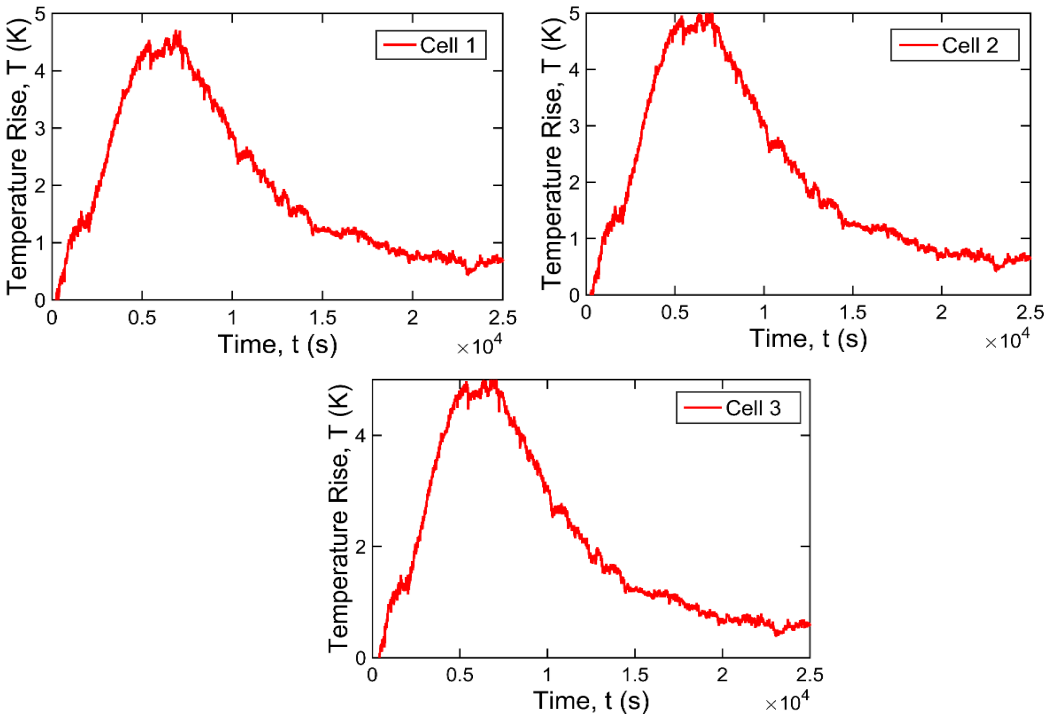

Figure 10: Image showing results during charging for cell 1, 2 and 3.

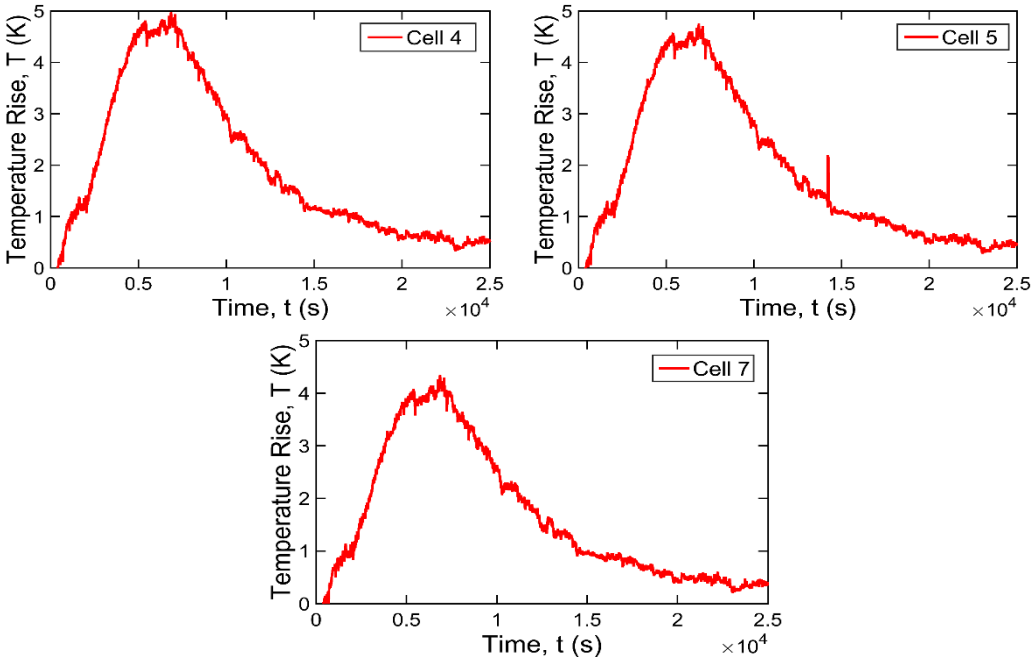

Figure 11: Image showing results during charging for cell 4, 5 and 7.

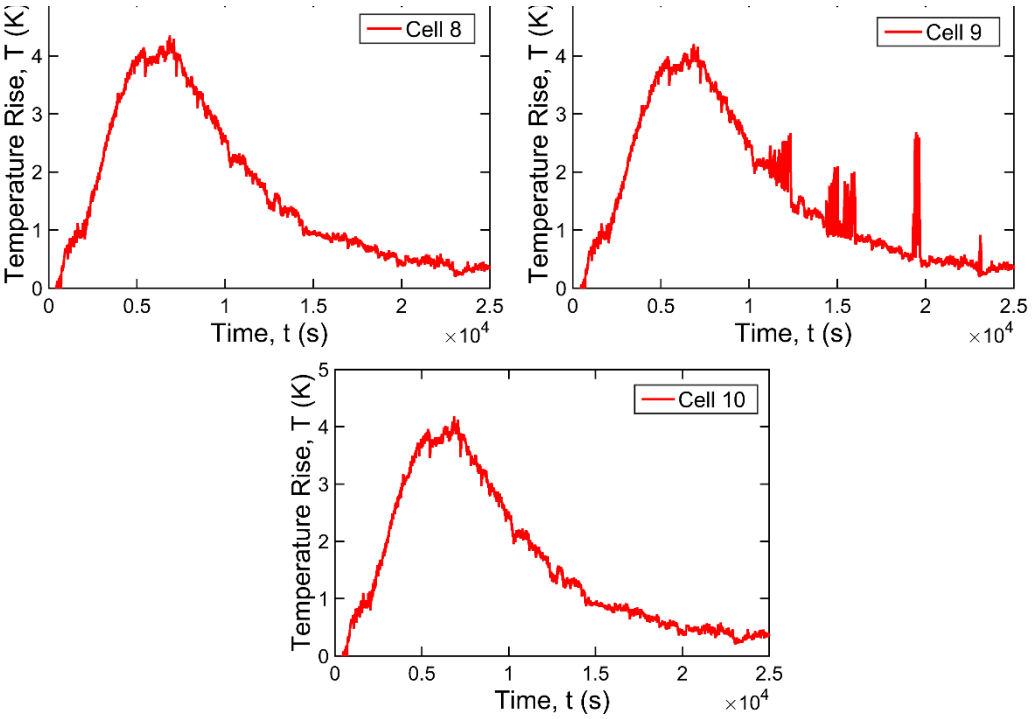

Figure 12: Image showing results during charging for cell 8, 9 and 10

5.2. Temperature Measurements with 30 Kg load and comparison with simulation model.

Experiment is performed with 30 Kg load by placing two stones on both accelerator pedal of the hoverboard. Experiment is performed at maximum speed of the hoverboard. After running at maximum speed, battery is discharged within 42 minutes, which is equivalent to 1.5C. This measurement is done only with natural convection case i.e. no grills. Figures 13, 14 and 15 show comparison plots of all cells for both experiment and simulation.

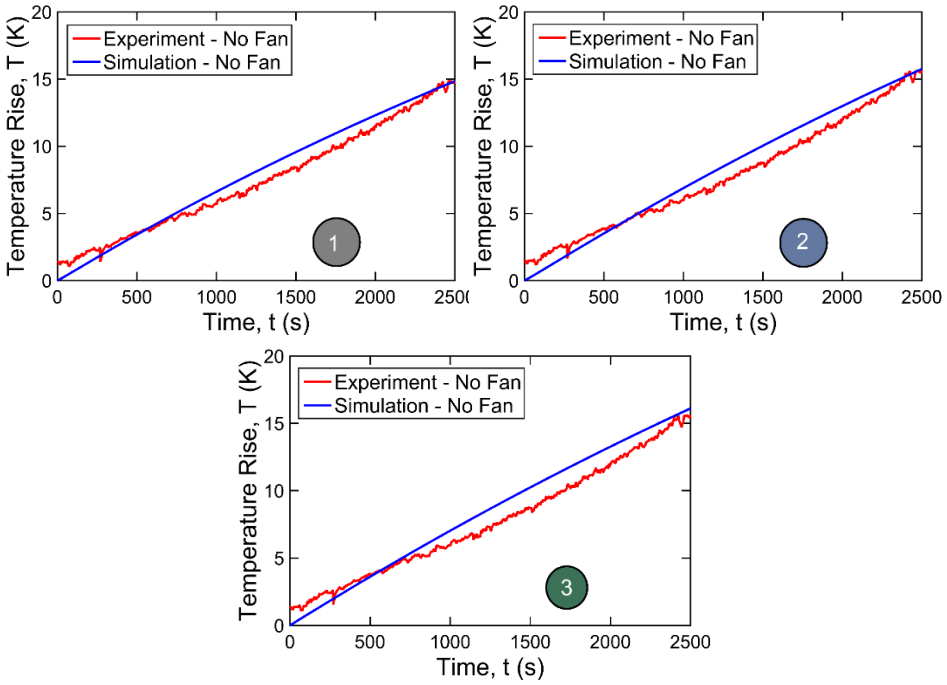

Figure 13: Comparison of experimentally measured temperature rise as a function of time with finite element simulation predictions for discharge at 1.5C rate. Comparison is shown for cells 1, 2 and 3 in the battery pack for natural convection case i.e. no grills.

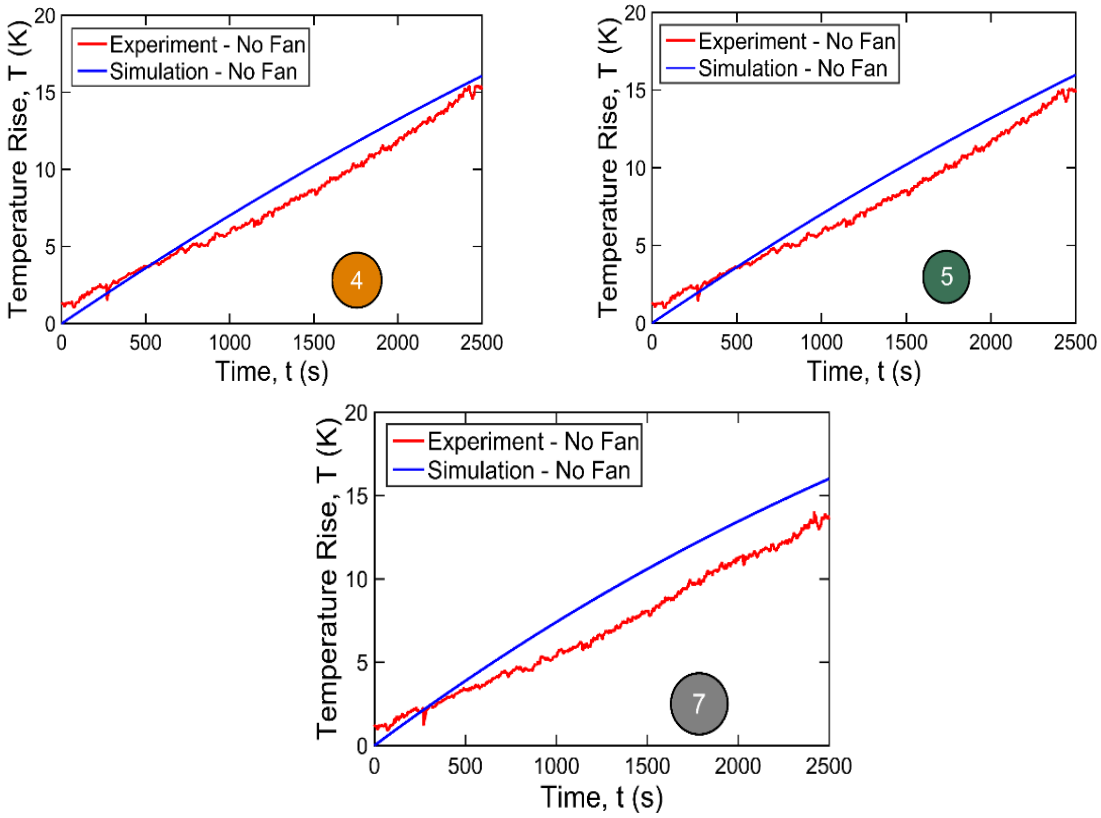

Figure 14: Comparison of experimentally measured temperature rise as a function of time with finite element simulation predictions for discharge at 1.5C rate. Comparison is shown for cells 4, 5 and 7 in the battery pack for natural convection case i.e. no grills.

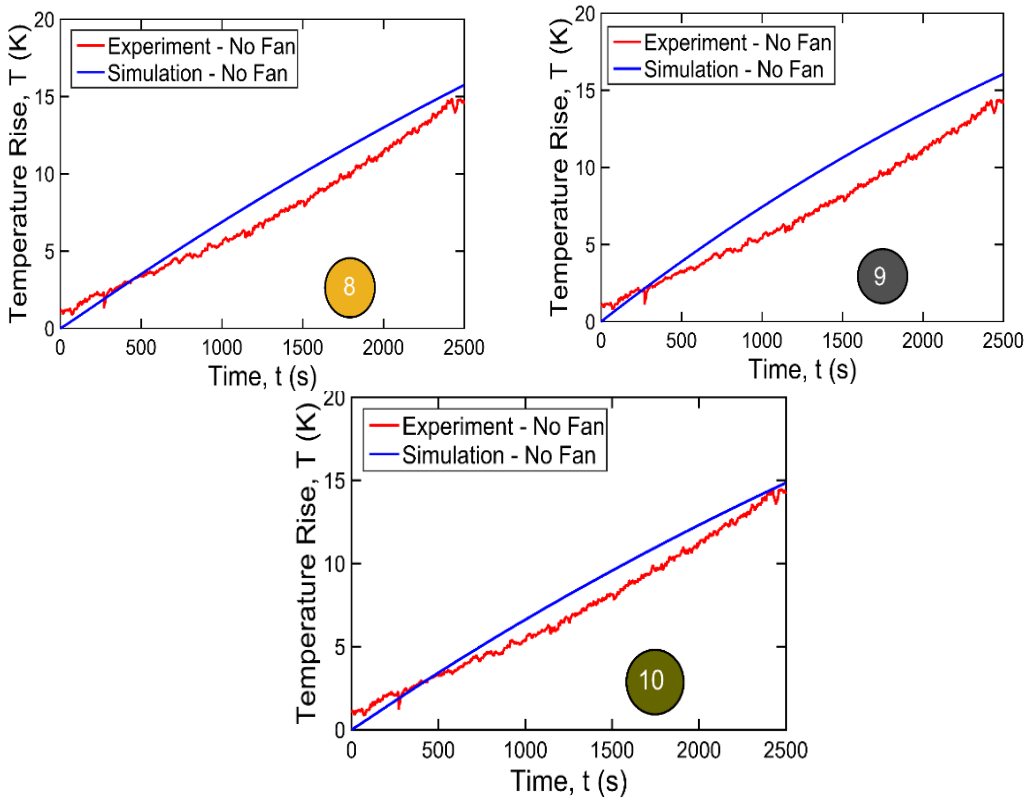

Figure 15: Comparison of experimentally measured temperature rise as a function of time with finite element simulation predictions for discharge at 1.5C rate. Comparison is shown for cells 8, 9 and 10 in the battery pack for natural convection case i.e. no grills.

5.3. Temperature Measurements with 70 Kg load

Figure 16 presents measured temperature rise at the surface of four cells in the battery pack during an aggressive hoverboard operation in which the entire battery pack is discharged within 15 minutes, which is the equivalent of 4C discharge rate. Positions of the cells within the battery pack are shown in Figure 2. Measurements are presented in two distinct cases. Figure 16(a) plots temperature for free convection conditions, wherein there is no forced air cooling and the cells are cooled only by free convection to the air around the battery pack. Figure 16(b) plots temperature in a similar discharge process in forced convection conditions due to air impinging on the battery pack from an external fan, as shown in Figure 7(b). Figure 16(a) shows, as expected, increasing temperature with time while the discharge process proceeds to completion. There is nearly uniform temperature rise among all four measured cells. The cell surface temperature increases by about 30 °C, which is a significant temperature rise. Such a large temperature rise is likely to cause performance and safety problems, particularly in a hot climate, since the manufacturer-specified safe temperature threshold for Li-ion cells is often only around 60-70 °C. Even though a well-designed battery management system is expected to limit the discharge rate to limit temperature rise, malfunction, poor design or operation in a challenging ambient may lead to the temperature rise measured here.

In contrast with Figure 16(a), experiments that mimic the cooling of the battery pack with air flow generated by hoverboard motion show substantial temperature reduction, as plotted in Figure 16(b). The benefit is particularly significant for cells 7 and 9 which are in the leading edge and trailing edge regions respectively. Peak temperature rise during forced convection reduces by half for cells 7 and 9 compared to the baseline case, which is a very significant reduction. While cell 7 benefits from direct impingement of the cooling air, the significant temperature reduction in cell 9 likely occurs due to air recirculation in the back of the battery pack. Cells 3 and 5, which are located on the side of the battery pack also benefit from cooling, although the benefit is lesser than cells 7 and 9.

Note that the four cells for which data are reported in Figure 4 represent different locations in the battery pack with respect to the cooling air flow. Temperature measurement for other cells, particularly those located in the inner region of the pack is not possible due to lack of accessibility. Temperature for such cells may be obtained from experimentally validated finite-element simulations as discussed in section 5.4. Further, data reported here are all surface temperatures, whereas the core temperature may be much greater

These experimental data establish the fundamental thermal benefit of using the air flow generated by hoverboard motion for cooling the battery pack. In harsh conditions, such as aggressive hoverboard operation in a high temperature ambient, the thermal benefit shown in Figure 16(b) may be sufficient enough to

prevent thermal runaway, or at least improve device reliability significantly. Note that the forced air convective cooling benefits shown here has not been optimized much in this study. Even greater temperature reduction than reported here may be possible, for example, by modifying the geometrical design of the cell arrangement within the battery pack, or the geometry around the battery pack. This is difficult to investigate in this work due to the lack of flexibility in making such changes in a commercial hoverboard.

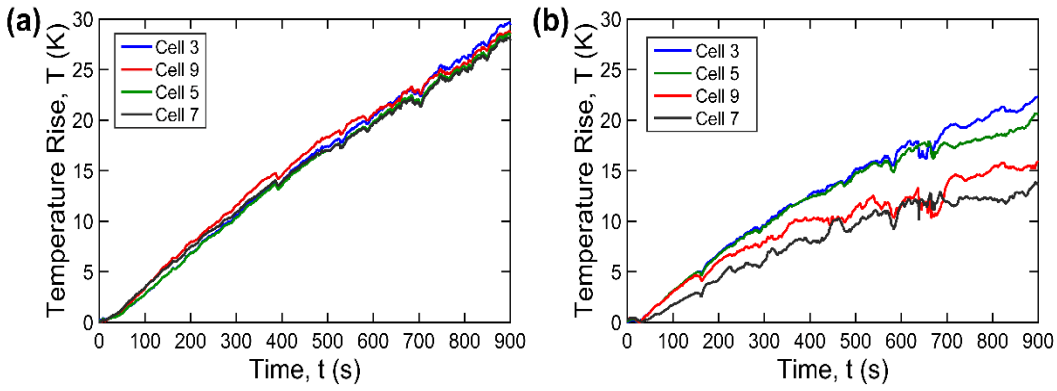

Figure 16: Experimental measurement of temperature rise as a function of time in four cells of battery pack during discharge at 4C rate. Measurements are shown in (a) free convection and (b) air cooled conditions

5.4. Simulation results and comparison with experimental data for 70 Kg load

It is clearly desirable to develop a finite-element simulation model for the temperature distribution in the hoverboard. This becomes particularly important because several cells in the battery pack are difficult to access for direct temperature measurement, and, also because the internal temperature of a cell is not possible to measure due to its hermetically sealed nature. In such a case, a model that predicts temperature inside the pack by accounting for the geometry of the battery pack and cooling conditions may be a valuable design tool. Validation of such a model against experimental data is critical as it increases confidence in model predictions.

Figure 17 presents a colormap of temperature distribution in the battery pack at the end of a 4C discharge rate in two different cooling conditions based on finite-element simulations described in Section 3. When the hoverboard operates in free convection conditions, significant temperature rise occurs in each cell of the battery pack, as shown in Figure 17(a). Temperature field is uniform among all cells, which is consistent with experimental data shown in Figure 16(a). The use of air flow generated by hoverboard motion results in substantial temperature reduction, as shown in Figure 17(b). There is some non-uniformity in the temperature map in this case, depending on cell location within the battery pack with respect to air flow. The improved temperature field in the battery pack may

contribute towards reduced risk of thermal runaway, as well as improved performance, since the reduced pack temperature can be leveraged to increase the discharge rate of the pack. However, the inter-cell non-uniformity induced due to convective cooling must also be accounted for by the battery management system.

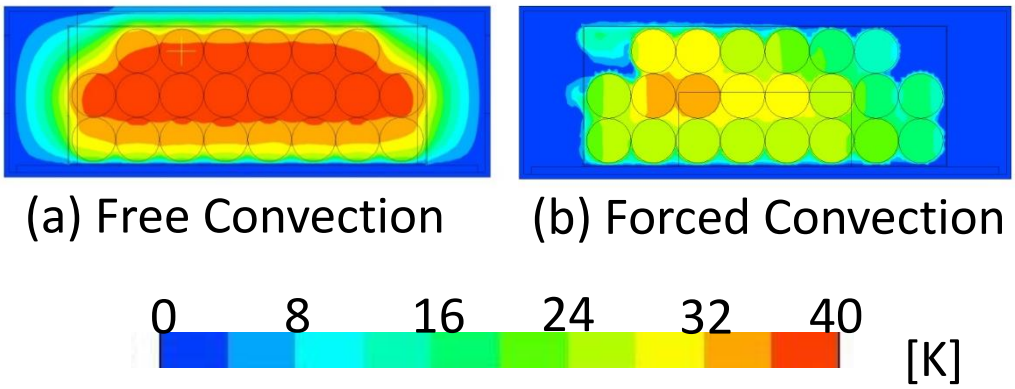

Figure 17: Colormap of temperature rise in the battery pack during discharge at 4C rate based on finite element simulations. Colormaps are shown for (a) free convection and (b) air cooled conditions.

Figures 18-20 present comparison of experimentally measured temperature rise as a function of time with finite element simulation results from 9 cells in the battery pack. Comparison is presented for both free convection conditions as well as forced convective cooling through a small fan. In each case, good agreement between experimental measurement and simulation results is observed. Temperature rise is lower for forced convection cooling compared to free

convection for each cell, as expected. Note that the nine cells for which results are presented in Figures 18, 19 and 20 represent distinct flow regions with respect to the inlet coolant air flow. While coolant air impinges directly on cell 7 and 8, cells 9 and 10 are located closer to the outlet grill, and cells 1, 2, 3, 4 and 5 are located on the bottom. The good agreement between simulation results and experimental data in different conditions for different cells validates the simulation model as a useful thermal design tool for understanding and optimizing the thermal characteristics of a hoverboard battery pack. For example, once validated, the model is capable of accurately predicting temperature for cells that are difficult to measure directly, such as cells in the internal region of the battery pack.

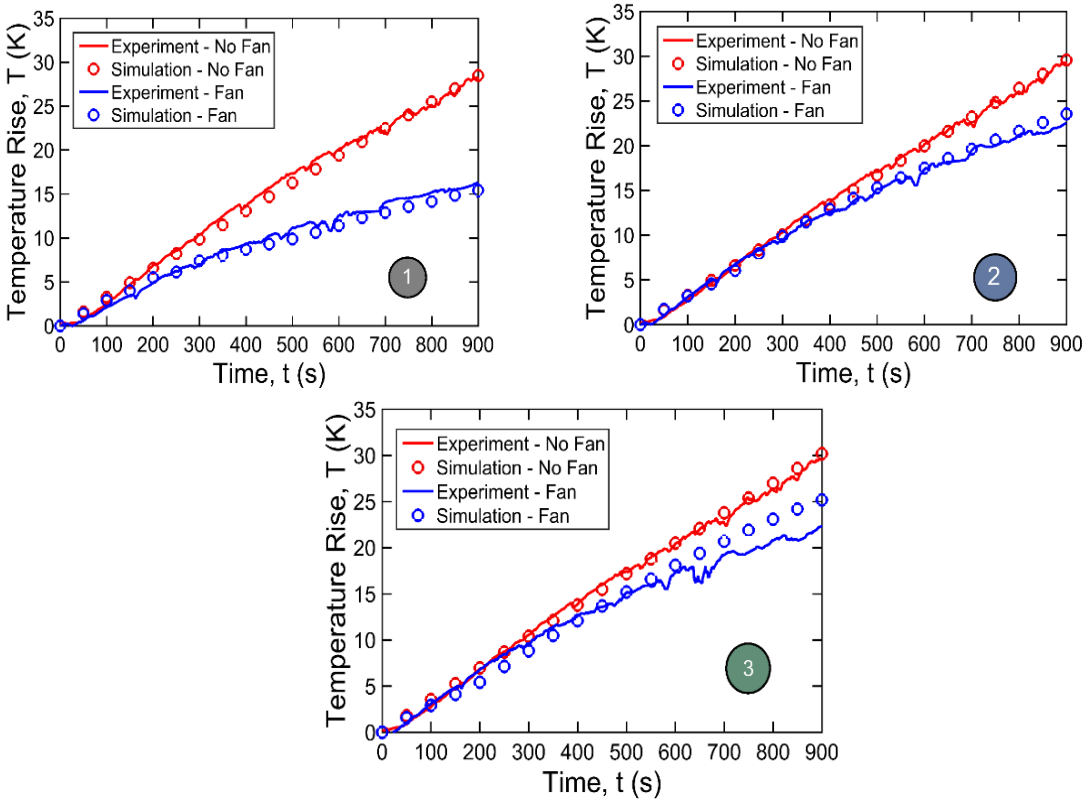

Figure 18: Comparison of experimentally measured temperature rise as a function of time with finite element simulation predictions for discharge at 4C rate. Comparison is shown for cells 1, 2 and 3 in the battery pack and for two different cooling conditions

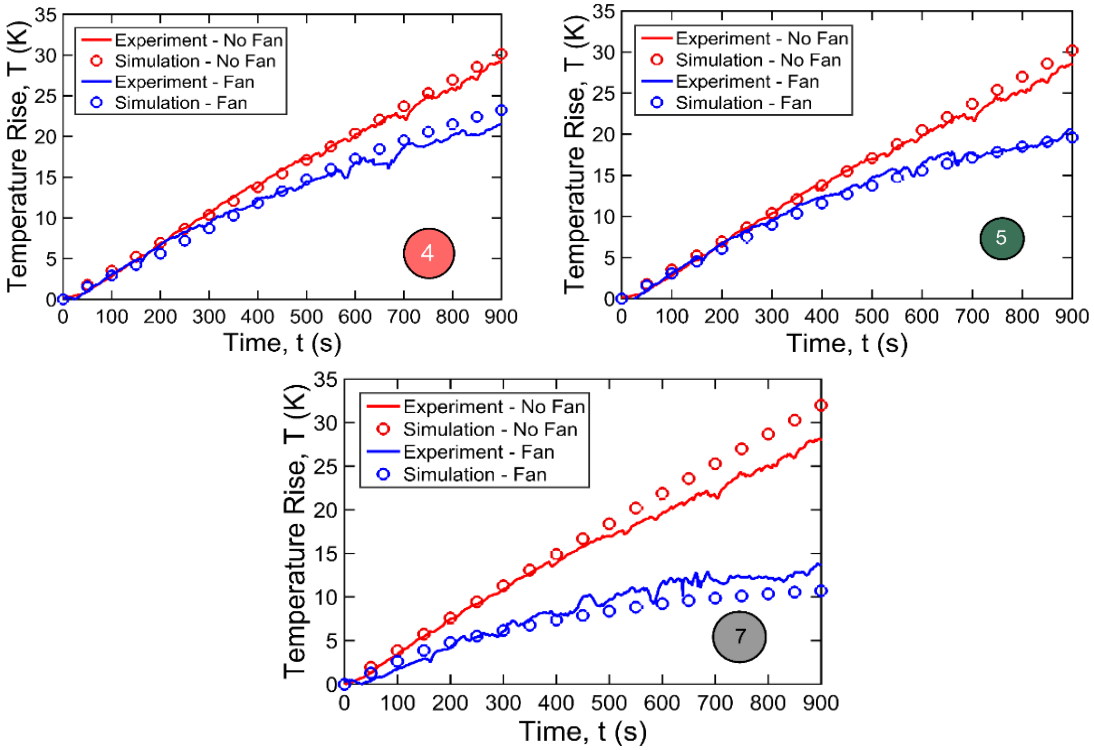

Figure 19: Comparison of experimentally measured temperature rise as a function of time with finite element simulation predictions for discharge at 4C rate. Comparison is shown for cells 4, 5 and 7 in the battery pack and for two different cooling conditions

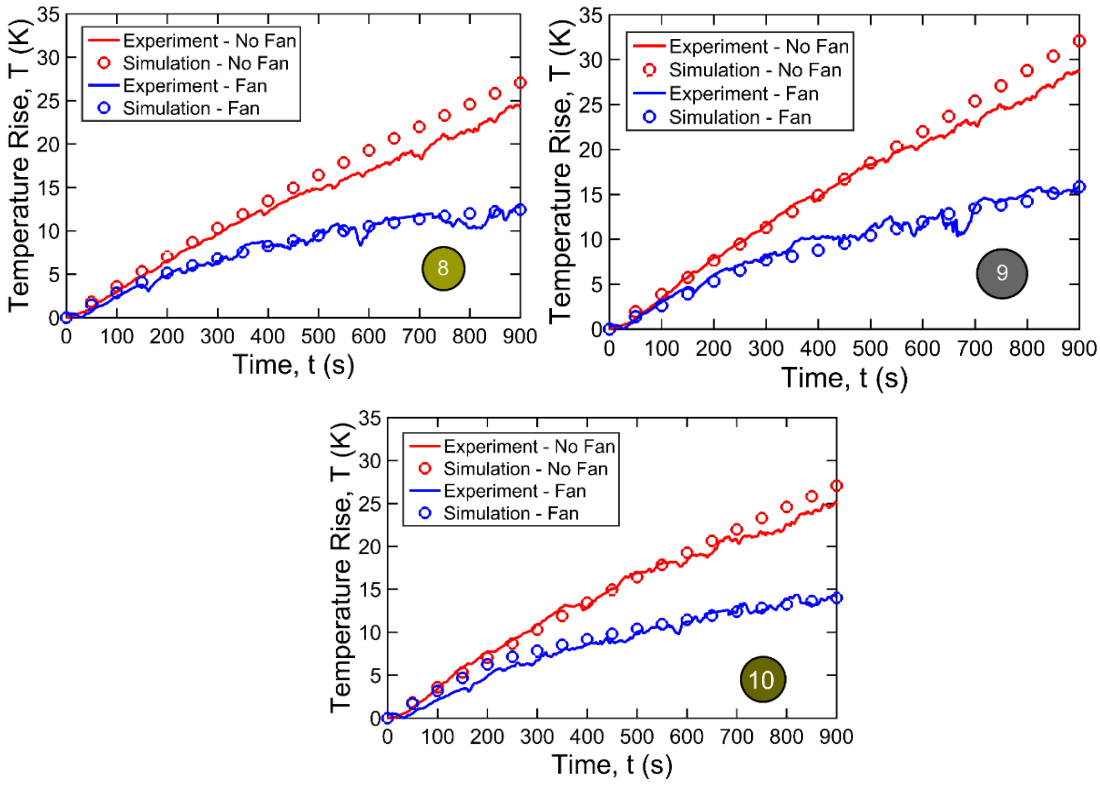

Figure 20: Comparison of experimentally measured temperature rise as a function of time with finite element simulation predictions for discharge at 4C rate. Comparison is shown for cells 8, 9 and 10 in the battery pack and for two different cooling conditions

The experimentally validated simulation model can predict thermal performance of the hoverboard battery pack in a variety of operating conditions. Figure 21 plots temperature rise in cell 5 as a function of time for multiple discharge rates in two different cooling conditions. These plots show that the cell temperature increases rapidly with increasing C-rate. In general, the greater the C-rate, the higher is the performance of the hoverboard. Plots such as those shown in Figure 21 help develop a trade-off between performance and thermal safety of the hoverboard battery pack.

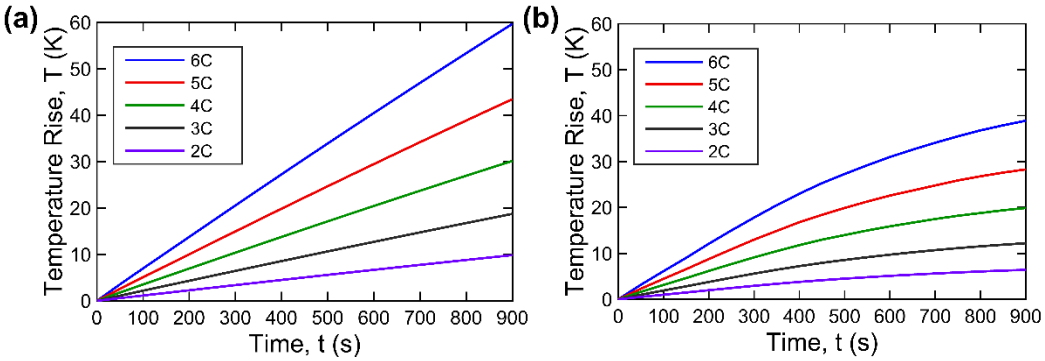

Figure 21: Plots of temperature rise of cell 5 as a function of time for multiple discharge rates in (a) free convection conditions, and (b) air cooled conditions.

5.5. Temperature prediction of middle cells from simulation model

While performing the experiment it is difficult to place thermocouples in the middle cells because of limited access to the middle cells, simulation model is used to predict the temperature of the middle cells. Figure 22 show temperature plot for cell “a”. Cell “a” is closer to the inlet grill, where there is direct impingement of cooling air. Because of its proximity to the inlet grill, temperature rise is comparatively less as compared to natural convection case, when there are no grills. There is 10 K temperature improvement, which is quite significant.

Figure 23 shows temperature plot for cell “b”. Cell “b” is away from the inlet grill and hence it does not have much access to the cooling air. There is an improvement of 5 K as compared to natural convection. Since cells are tightly packed, there is not much improvement in the cells which are away from inlet grill. In forced convection case, contour plot in Figure 17, cells which are away from inlet grill are hotter compared to cells which are closer to grills. Packaging of cells plays an important factor in thermal management of the battery pack.

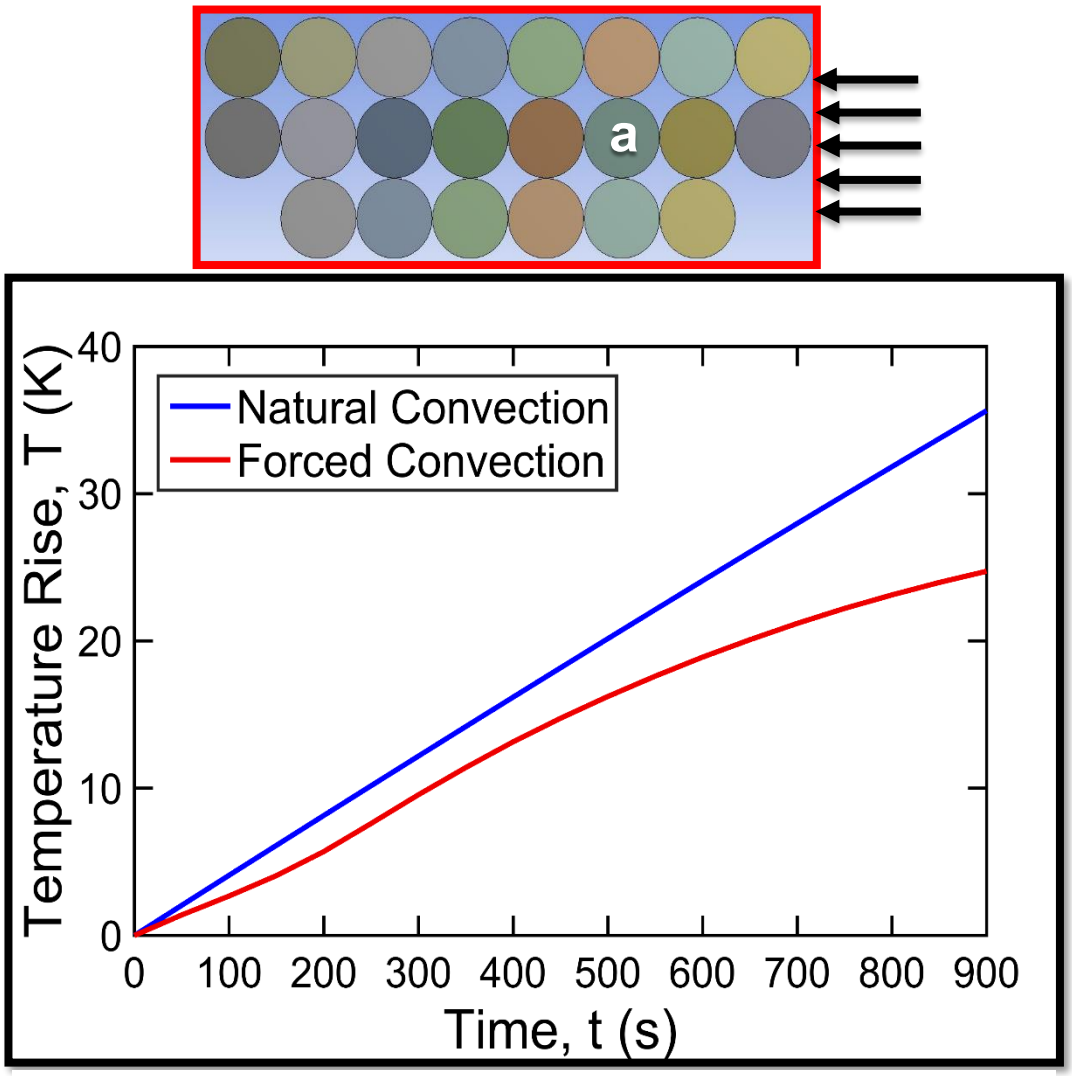

Figure 22: Plot of temperature rise of cell “a” as a function of time for natural convection conditions and forced cooled conditions.

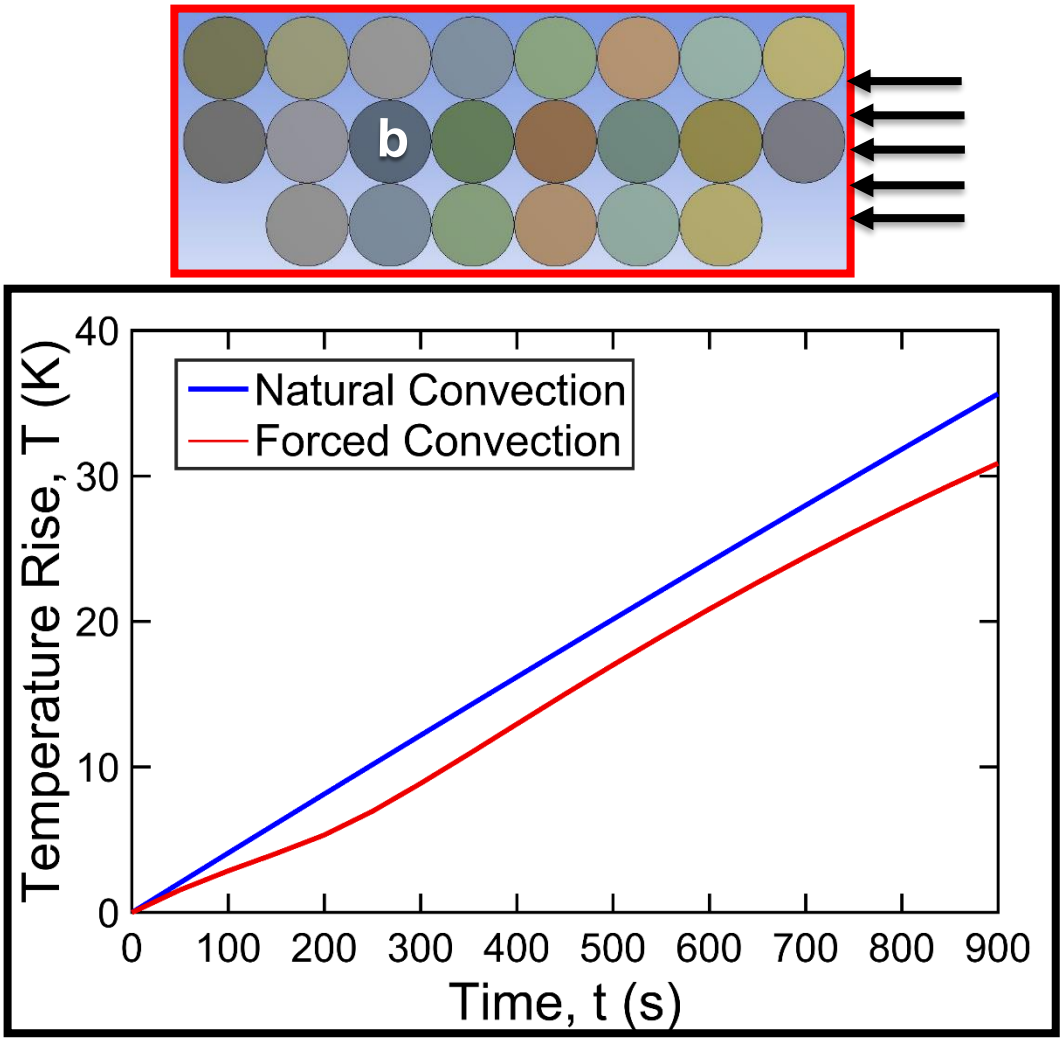

Figure 23: Plot of temperature rise of cell "b" as a function of time for natural convection and forced convection conditions

5.6. Effect of metal casing on thermal management

The battery pack in the hoverboard is protected from external abuse and impact by a metal casing, as shown in Figure 2. However, it is likely to adversely impact forced convection cooling of cells in the battery pack by isolating the cells from the air flow. A set of experiments is carried out to examine this challenge in detail and investigate a possible solution.

Figure 24 plots temperature of cell 5 as a function of time during 4C discharge for three different conditions related to the metal casing. As a baseline, temperature in presence of the metal casing and with no air flow is plotted. This represents the present state-of-the-art in a hoverboard battery pack, wherein the cells in the pack cool down only through natural convection. Temperature is also plotted for the case of air flow with the metal casing present. A comparison of these two plots shows that while air flow from the fan reduces temperature rise, the effect is not significant, primarily because the presence of the metal casing prevents direct impingement of air flow on the cells, and therefore severely limits the benefit of convective cooling. Experimental data are also plotted in Figure 24 for the case where the metal casing is removed completely in addition to providing air flow. A significantly greater thermal benefit is obtained in this case, with a nearly 33% reduction in measured temperature at the end of the discharge process compared to the baseline case. Finite element simulations of these cases confirm, as

expected, that the removal of the metal casing facilitates direct impingement of coolant flow on the cells in the battery pack, and therefore, more effective cooling.

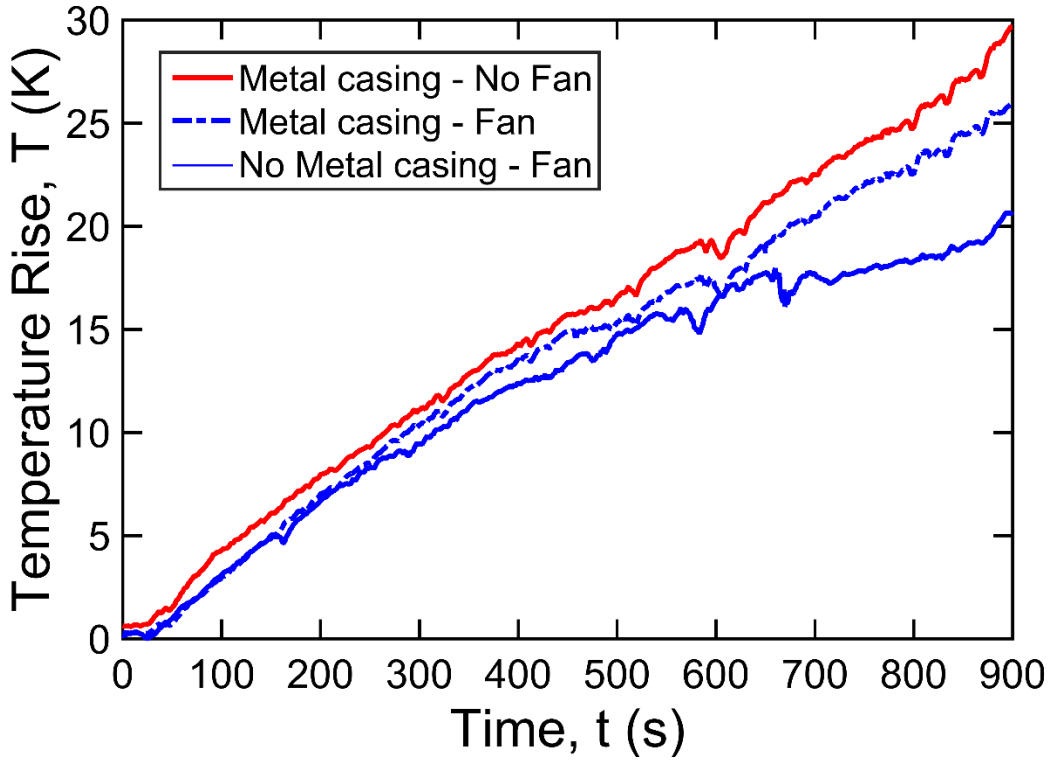

Figure 24: Experimentally measured temperature rise in cell 5 as a function of time for the baseline case and for air cooling without and with the metal casing, showing that the effect of cooling is more pronounced in the absence of the metal casing which facilitates direct air impingement on the battery pack

Despite the significant thermal benefit of removing the metal casing completely, it may not always be possible to do so, because the casing protects the battery pack from external impacts and possibly also serves a structural function. As an alternative to completely removing the metal casing, the possibility of providing greater air flow into the battery pack through perforations in the metal casing is investigated through simulations. Figure 25 plots temperature rise in cell 5 during 4C discharge for the baseline case of no fan. In addition, the thermally beneficial, but perhaps impractical case of removing the metal casing completely while providing air flow is also plotted.

For comparison, finite element simulations are carried out for the case where two perforations of dimension 55 mm by 35 mm are provided on the front and back surfaces of the metal casing. Temperature distribution for this case, also plotted in Figure 25 clearly shows that the thermal benefit in this case is nearly as much as the case where the metal casing is removed completely. This may present a reasonable compromise in designing thermal management of the battery pack while keeping the metal casing in place. Perforations in the metal casing permit significant air flow through, without adversely impacting the structural function of the casing.

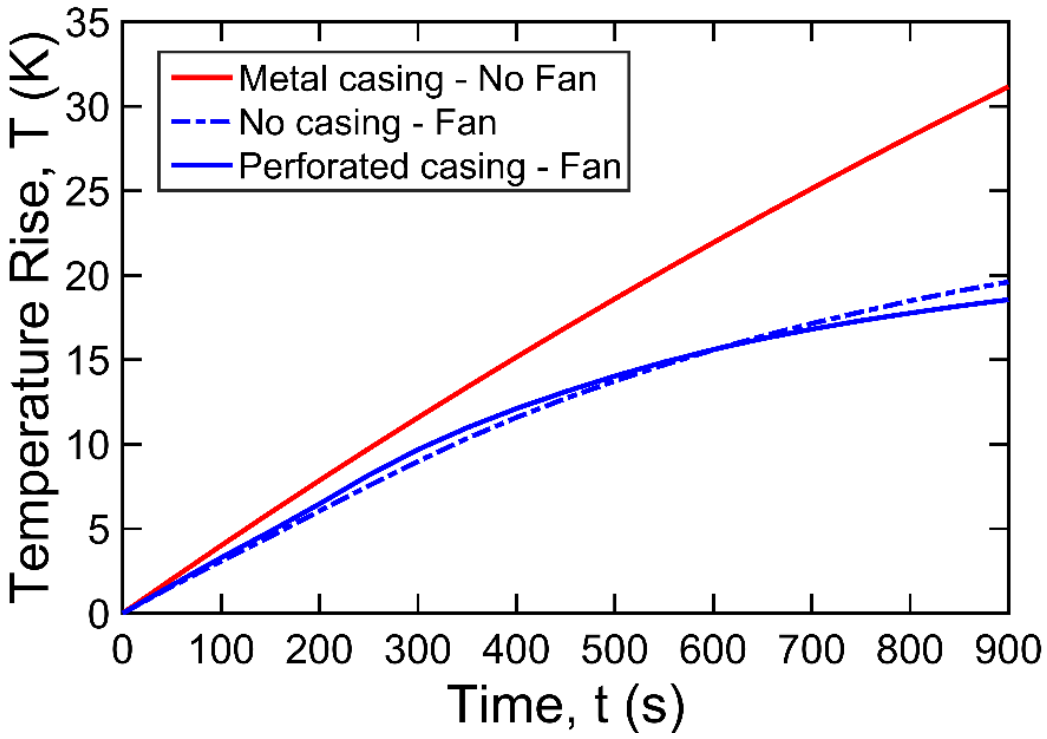

Figure 25: Temperature rise as a function of time in cell 5 during discharge at 4C rate based on finite element simulations. Comparison is made between the baseline case, air cooling without the metal casing at all, and air cooling with a perforated metal casing

Chapter 6

Conclusion

Results discussed above present critical insights into heat transfer processes in the battery pack of a hoverboard. Multiple recent fires and accidents in hoverboards are known to have originated in the battery pack of the hoverboard. While hoverboards have not received as much research attention as electric vehicles, ensuring the safety of hoverboards is nevertheless very critical due to their widespread use and the limited available thermal management design space. Experimental measurements presented here highlight the importance of active cooling, particularly in aggressive operating conditions. Cooling with the air stream around the hoverboard during motion is mimicked in experiments, and is shown to result in significant temperature reduction, with the possibility of even greater benefit through flow and thermal optimization. Experimental data also highlight the important role of the metal casing around the battery pack in thermal management. These results also indicate the possibility of a trade-off between thermal management and structural function of the metal casing wherein a perforated casing may offer extensive thermal benefit without compromising its structural function. The experimentally validated simulation models discussed in this work offer a useful design tool for battery pack thermal management in a

hoverboard. Thermal optimization based on such a tool may lead to safer, higher performance hoverboards.

Chapter 7

Future Work

Cells in battery pack of a hoverboard are tightly packed. Many cells don't have physical access to the cooling air. As shown in Figure 23, even if by providing grills temperature improvement in the inner cells are only 5 K as compared to natural convection. To improve thermal management in battery packs, orientation of the cells can be changed. By implementing this, every cell will get access to the cooling air and it might help in improving the thermal management of the battery pack.

Experiments can also be done by using passive cooling techniques such as phase change material. Because of large latent heat associated with phase change, significant amount of heat removal rate is possible. Using phase change material in battery pack of hoverboard can give an interesting insight on thermal management of the cell.

BIOGRAPHY

Abhinav Prasad received his bachelor's degree in Mechanical Engineering from ITER, Bhubaneswar, India, in the year 2011. He worked in an automotive industry for four and a half years as a thermal systems design engineer. He pursued his Master's in Mechanical Engineering in University of Texas at Arlington from Fall 2016. He joined Microscale Thermophysics laboratory and started working with Dr. Ankur Jain in 2017. His research interest includes battery thermal modelling and powertrain thermal design.

Contact: abhinav.prasad@mavs.uta.edu

References:

[1] K. Shah, N. Balsara, S. Banerjee, M. Chintapalli, A.P. Cocco, W.K.S. Chiu, et al., State of the Art and Future Research Needs for Multiscale Analysis of Li-Ion Cells, J. Electrochem. Energy Conv. & Storage 14 (2017) 020801. https://doi.org/10.1115/1.4036456.

[2] B. Scrosati, J. Garche, Lithium batteries: Status, prospects and future, J. Power Sources 195 (2010) 2419–2430. https://doi.org/10.1016/j.jpowsour.2009.11.048

[3] V. Etacheri, R. Marom, R. Elazari, G. Salitra, D. Aurbach, Challenges in the development of advanced Li-ion batteries: a review, Energy & Environ. Sci. 4 (2011) 3243. https://doi.org/10.1039/C1EE01598B

[4] D. Linden, T.B. Reddy, 'Handbook of Batteries', 3rd Ed., McGraw-Hill, New York, 2002.

[5] K. Shah, V. Vishwakarma, A. Jain, Measurement of Multiscale Thermal Transport Phenomena in Li-Ion Cells: A Review, J. Electrochem. Energy Conv. & Storage 13 (2016) 030801. https://doi.org/10.1115/1.4034413.

[6] T.M. Bandhauer, S. Garimella, T.F. Fuller, A Critical Review of Thermal Issues in Lithium-Ion Batteries, J. Electrochem. Soc. 158 (2011). https://doi.org/10.1149/1.3515880.

[7] K. Shah, D. Chalise, A. Jain, Experimental and theoretical analysis of a method to predict thermal runaway in Li-ion cells, J. Power Sources. 330 (2016) 167–174. https://doi.org/10.1016/j.jpowsour.2016.08.133

[8] C.F. Lopez, J.A. Jeevarajan, P.P. Mukherjee, Characterization of Lithium-Ion Battery Thermal Abuse Behavior Using Experimental and Computational Analysis, J. Electrochem. Soc. 162 (2015). https://doi.org/10.1149/2.0751510jes.

[9] S. Drake, D. Wetz, J. Ostanek, S. Miller, J. Heinzel, A. Jain, Measurement of anisotropic thermophysical properties of cylindrical Li-ion cells, J. Power Sources. 252 (2014) 298–304. https://doi.org/10.1016/j.jpowsour.2013.11.107

[10] S. Drake, M. Martin, D. Wetz, J. Ostanek, S. Miller, J. Heinzel, et al., Heat generation rate measurement in a Li-ion cell at large C-rates through temperature and heat flux measurements, J. Power Sources 285 (2015) 266–273. https://doi.org/10.1016/j.jpowsour.2015.03.008

[11] K. Shah, D. Chalise, A. Jain, Experimental and theoretical analysis of a method to predict thermal runaway in Li-ion cells, J. Power Sources 330 (2016) 167–174. https://doi.org/10.1016/j.jpowsour.2016.08.133

[12] J. Zhang, B. Wu, Z. Li, J. Huang, Simultaneous estimation of thermal parameters of large- format laminated Lithium-Ion Batteries, J. Power Sources 259 (2014) 106-116. http://doi.org/10.1016/j.jpowersour.2014.02.079.

[13] C.F. Lopez, J.A. Jeevarajan, P.P. Mukherjee, Evaluation of Combined Active and Passive Thermal Management Strategies for Lithium-Ion Batteries, Journal of Electrochemical Energy Conversion and Storage. 13 (2016) 031007. http://doi.org/10.1115/1.4035245.

[14] S.A. Khateeb, S. Amiruddin, M. Farid, J.R. Selman, and S.A. Hallaj. Thermal management of Li-ion battery with phase change material for electric scooters: experimental validation, J. Power Sources 142 (2005) 345-353. https://doi.org/10.1016/j.jpowsour.2004.09.033

[15] M.D. Zolot, K. Kelly, M. Keyser, M. Mihalic, A. Pesaran, A. Hieronymus, 'Thermal evaluation of the Honda Insight battery pack', In: 36th ASME Intersoc. Energy Conv. Eng. Conf., 2001, pp. 923.

[16] M. Zolot, A. Pesaran, M. Mihalic, 'Thermal evaluation of Toyota Prius battery pack,' In: Proc. Future Car Congress, 2002.

[17] D. Macneil, Z. Lu, Z. Chen, J. Dahn, A comparison of the electrode/electrolyte reaction at elevated temperatures for various Li-ion battery cathodes, J. Power Sources 108 (2002) 8–14. https://doi.org/10.1016/S0378-7753(01)01013-8

[18] R. Spotnitz, J. Franklin, Abuse behavior of high-power, lithium-ion cells, J. Power Sources 113 (2003) 81–100.

https://doi.org/10.1016/S0378-7753(02)00488-3

[19] A.W. Golubkov, D. Fuchs, J. Wagner, H. Wiltsche, C. Stangl, G. Fauler, et al., Thermal-runaway experiments on consumer Li-ion batteries with metal-oxide and olivin-type cathodes, RSC Adv. 4 (2014) 3633–3642. https://doi.org/10.1039/C3RA45748F

[20] M. Parhizi, M. Ahmed, A. Jain, Determination of the core temperature of a Li-ion cell during thermal runaway, J. Power Sources 370 (2017) 27–35. https://doi.org/10.1016/j.jpowsour.2017.09.086

[21] G. Karimi, X. Li, Thermal management of lithium-ion batteries for electric vehicles, International Journal of Energy Research. 37 (2012) 13–24.https://doi.org/10.1002/er.1956.

[22] Z. Qian, Y. Li, Z. Rao, Thermal performance of lithium-ion battery thermal management system by using mini-channel cooling, Energy Conversion & Management 126 (2016) 622–631. https://doi.org/10.1016/j.enconman.2016.08.063

[23] R. Zhao, S. Zhang, J. Gu, J. Liu, S. Carkner, E. Lanoue, An experimental study of lithium ion battery thermal management using flexible hydrogel films, J. Power Sources. 255 (2014) 29–36. https://doi.org/10.1016/j.jpowsour.2013.12.138

[24] J. Zhao, Z. Rao, Y. Li, Corrigendum to “Thermal performance of mini-channel liquid cooled cylinder based battery thermal management for cylindrical lithium-ion power battery” [Energy Convers. Manage. 103 (2015) 157–165], Energy Conversion and Management. 155 (2018) 346. https://doi.org/10.1016/j.enconman.2015.06.056

[25] S.A. Khateeb, M.M. Farid, J. Selman, S. Al-Hallaj, Design and simulation of a lithium-ion battery with a phase change material thermal management system for an electric scooter, J. Power Sources 128 (2004) 292–307. https://doi.org/10.1016/j.jpowsour.2003.09.070

[26] M. Parhizi, A. Jain, Analytical modelling and optimization of phase change thermal management of Li-ion battery pack, Applied Energy, in review (2018).

[27] Z. Ling, F. Wang, X. Fang, X. Gao, Z. Zhang, A hybrid thermal management system for lithium ion batteries combining phase change materials with forced-air cooling, Appl. Energy 148 (2015) 403–409. https://doi.org/10.1016/j.apenergy.2015.03.080

[28] Z. Rao, S. Wang, M. Wu, Z. Lin, F. Li, Experimental investigation on thermal management of electric vehicle battery with heat pipe, Energy Conversion and Management. 65 (2013) 92–97. https://doi.org/10.1016/j.enconman.2012.08.014

[29] Y. Ye, Y. Shi, L.H. Saw, A.A. Tay, Performance assessment and optimization of a heat pipe thermal management system for fast charging lithium ion battery packs, Int. J. Heat & Mass Transfer 92 (2016) 893–903. https://doi.org/10.1016/j.ijheatmasstransfer.2015.09.052

[30] A. Mills, S.A. Hallaj. Simulation of passive thermal management system for lithium-ion battery packs, J. Power Sources 141 (2005) 307-315. https://doi.org/10.1016/j.jpowsour.2004.09.025

[31] S.A. Hallaj, Said, H. Maleki, J.S. Hong, and J.R. Selman, Thermal modeling and design considerations of lithium-ion batteries, J. Power Sources 83 (1999) 1-8. https://doi.org/10.1016/S0378-7753(99)00178-0

[32] Y. Ye, L.H. Saw, Y. Shi, A.A. Tay, Numerical analyses on optimizing a heat pipe thermal management system for lithium-ion batteries during fast charging, Appl. Thermal Eng. 86 (2015) 281–291. https://doi.org/10.1016/j.applthermaleng.2015.04.066

[33] D. Anthony, D. Wong, D. Wetz, A. Jain, Non-invasive measurement of internal temperature of a cylindrical Li-ion cell during high-rate discharge, International Journal of Heat and Mass Transfer. 111 (2017) 223–231. http://doi.org/10.1016/j.ijheatmasstransfer.2017.03.095.

[34] M. Parhizi, M. Ahmed, A. Jain, Determination of the core temperature of a Li-ion cell during thermal runaway, Journal of Power Sources. 370 (2017) 27–35. https://doi.org/10.1016/j.jpowsour.2017.09.086.